HHS Public Access

Author manuscript

Phys Med Biol. Author manuscript; available in PMC 2017 September 21.

Published in final edited form as:

Phys Med Biol. 2016 September 21; 61(18): L38–L47. doi:10.1088/0031-9155/61/18/L38.

Bismuth germanate coupled to near ultraviolet silicon photomultipliers for time-of-flight PET

Sun Il Kwon[1,3], **Alberto Gola**[2], **Alessandro Ferri**[2], **Claudio Piemonte**[2], and **Simon R. Cherry**[1]

[1]Department of Biomedical Engineering, University of California, Davis, Davis, CA 95616, USA

[2]Fondazione Bruno Kessler, Trento, Italy

Abstract

Bismuth germanate (BGO) was a very attractive scintillator in early-generation positron emission tomography (PET) scanners. However, the major disadvantages of BGO are lower light yield and longer rise and decay time compared to currently popular scintillators such as LSO and LYSO. This results in poorer coincidence timing resolution and it has generally been assumed that BGO is not a suitable scintillator for time-of-flight (TOF) PET applications. However, when a 511-keV photon interacts in a scintillator, a number of Cerenkov photons are produced promptly by energetic electrons released by photoelectric or Compton interactions. If these prompt photons can be captured, they could provide a better timing trigger for PET. Since BGO has a high refractive index (increasing the Cerenkov light yield) and excellent optical transparency down to 320 nm (Cerenkov light yield is higher at shorter wavelengths), we hypothesized that the coincidence timing resolution of BGO can be significantly improved by efficient detection of the Cerenkov photons. However, since the number of Cerenkov photons is far less than the number of scintillation photons, and they are more abundant in the UV and blue part of the spectrum, photosensors need to have high UV/blue sensitivity, fast temporal response, and very low noise in order to trigger on the faint Cerenkov signal. In this respect, NUV-HD silicon photomultipliers (SiPMs) (FBK, Trento, Italy) are an excellent fit for our approach. In this study, coincidence events were measured using BGO crystals coupled with NUV-HD SiPMs. The existence and influence of Cerenkov photons on the timing measurements were studied using different configurations to exploit the directionality of the Cerenkov emissions. Coincidence resolving time values (FWHM) of ~270 ps from 2 × 3 × 2 mm^3 BGO crystals and ~560 ps from 3 × 3 × 20 mm^3 BGO crystals were obtained. To our knowledge, these are the best coincidence resolving time values reported for BGO to date. With these values, BGO can be considered as a relevant scintillator for TOF PET scanners, especially if photodetectors with even better near UV/blue response can be developed to further improve the efficiency of Cerenkov light detection.

1. Introduction

Bismuth germanate (BGO) was a very attractive scintillator in early-generation positron emission tomography (PET) scanners (Rota Kops *et al* 1990, Wienhard *et al* 1992, Wienhard *et al* 1994, DeGrado *et al* 1994) since it has a short attenuation length (1.1 cm) for 511 keV

[3]Author to whom correspondence should be addressed. sunkwon@ucdavis.edu.

gamma rays due to its high effective atomic number and density (Melcher 2000, Humm *et al* 2003, Moses 2007). However, the disadvantages of BGO are lower light yield and longer rise and decay time compared to lutetium oxyorthosilicate (LSO) and lutetium-yttrium oxyorthosilicate (LYSO) scintillators (Humm *et al* 2003, Pepin *et al* 2004, Moses 2007). These result in degradation of energy resolution and coincidence timing resolution. Previous studies reported a coincidence timing resolution of ~1.5 ns for 20-mm-long BGO crystals (Moses 2007, Szczesniak *et al* 2013). For this reason, it has been assumed that BGO is not suitable for time-of-flight (TOF) PET applications where the timing information is used to improve image quality (Karp *et al* 2008, Surti 2015) and requires timing resolution better than ~600 picoseconds.

When a 511-keV annihilation photon interacts in a scintillator, a small number of optical Cerenkov photons are produced promptly by energetic electrons released by photoelectric or Compton interactions. This prompt light should provide a better timing trigger for PET (Williams *et al* 2001, Lecoq *et al* 2010, Korpar *et al* 2011, Brunner *et al* 2014, Dolenec *et al* 2016). Since BGO has a high refractive index (2.15) and excellent optical transparency down to 320-nm (Rihua *et al* 2008), more Cerenkov photons can be produced and traverse the scintillator compared to other scintillators where either the Cerenkov light production is lower, or much of the Cerenkov light is absorbed within the crystal. Consequently, we hypothesized that the coincidence timing resolution of BGO can be much improved by efficiently detecting these Cerenkov photons, while scintillation photons are still used for determining energy information. However, the number of Cerenkov photons is very small compared to the scintillation photons (Williams *et al* 2001, Lecoq *et al* 2010, Korpar *et al* 2011, Brunner *et al* 2014). For BGO, the energy threshold for an energetic electron to emit Cerenkov photons is about 66 keV given the refractive index of 2.15. The estimated number of produced Cerenkov photons produced per photoelectric interaction is ~15.6 over a wavelength range of 320 nm to 800 nm (Lecoq *et al* 2010, Somlai-Schweiger and Ziegler 2015). Therefore, photosensors for this approach need to have high UV/blue sensitivity (the Cerenkov signal is heavily weighted towards shorter wavelengths), fast temporal response, and very low noise in order to trigger on the faint but prompt Cerenkov signal. Recently, FBK (Trento, Italy) developed a high-density cell silicon photomultiplier (SiPM) technology for UV and blue light detection, named NUV-HD SiPM. This SiPM shows excellent timing resolution, high photodetection efficiency (PDE) across the spectrum, especially in the UV/blue, and low noise (Piemonte *et al* 2016). These features are well suited with our goal of efficiently detecting both Cerenkov and scintillation photons. In this study, we show remarkable improvement in the coincidence timing resolution of BGO coupled with NUV-HD SiPMs by using the Cerenkov photons for timing and scintillation photons for energy.

2. Materials and methods

2.1. BGO scintillators and SiPMs

Two polished 3 × 3 × 20 mm^3 BGO pixels (Hilger Analytical, Margate, UK), corresponding to a relevant size for clinical PET, were prepared and wrapped in three layers of polytetrafluoroethylene (PTFE) tape. Two smaller 2 × 3 × 2 mm^3 BGO pixels were also prepared, with the two square surfaces (2 × 2 mm^2) roughened, while all other surfaces (2 ×

3 mm^2) were polished. One of the 2 × 3 mm^2 surfaces was coupled to the SiPM. Each small BGO pixel was encased by a black painted holder that was made by a 3D printer (Object 260, Stratasys, Ltd.) using acrylate-based photo-polymers (VeroWhite).

Two NUV-HD SiPMs and two RGB-HD SiPMs developed by FBK with a sensitive area of 4 × 4 mm^2 were used for coincidence measurements. The NUV-HD SiPMs used in this study have a square cell pitch of 40 μm and a fill factor of ~83%. The PDE spectrum of the NUV-HD SiPMs peaks at 400-420 nm with a maximum value of 60% at 10.3 V overvoltage. The PDE between 300 nm and 400 nm is still over 45%. The more conventional RGB-HD SiPMs (Piemonte *et al* 2013) feature a broad and high PDE across the visible light region with a maximum value close to 50% at 500-550 nm at 9 V over voltage. The RGB-HD SiPMs used in this study have a square cell pitch of 25 μm and a fill factor of ~70%. Figure 1 shows the PDE of NUV-HD and RGB-HD SiPMs as a function of wavelength as well as the emission spectrum of BGO and the spectrum of Cerenkov luminescence.

Silicone optical grease (BC-630, Saint-Gobain) was used for optical coupling between BGO pixels and SiPMs. It has a refractive index of 1.465 and a very flat transmittance of ~ 95% for wavelengths down to 280 nm.

2.2. Coincidence measurement setup

We first characterized one pair of detectors composed of 3 × 3 × 20 mm^3 BGO pixels coupled to NUV-HD SiPMs. Coincidence events from the two 511-keV annihilation gamma rays emitted by a ^{22}Na point source were measured using the coincidence measurement setup shown in figure 2(a). A total of 13,500 coincidence events were stored in each BGO and photosensor pair. Each SiPM was connected to a custom amplifier. The amplifier had two outputs: an energy output used to calculate the energy of each event and a timing output filtered with a pole-zero cancellation circuit, which reduced the baseline fluctuation produced by pileup of dark events, and was used to calculate coincidence timing resolution (Gola *et al* 2013). Output signals were digitized with an oscilloscope (DPO 7254, Tektronix) at a sampling rate of 10 GS/s. Coincidence events were determined by a coincidence logic unit using energy signals. The bias voltages of all SiPMs were optimized and set to an overvoltage of 10 V and 9.5 V for the NUV-HD and RGB-HD SiPMs, respectively. Timing signals from the amplifiers were directly coupled to the input channels in the oscilloscope. To reduce quantization noise, a vertical scale of 10 mV/Div was set in the oscilloscope for the timing signals (Gola *et al* 2013). The temperature of the detectors was maintained at 20 ° by supplying chilled air.

To examine the influence of Cerenkov photons, coincidence events were measured using head-to-head (H2H) and back-to-back (B2B) configurations as shown in figure 2(b) and (c), respectively. Theoretically, energetic electrons are mostly ejected in the forward direction (relative to the incident direction of 511-keV photons). Even after scattering of the electrons, this results in a modest preferential production of Cerenkov photons in the forward direction. This phenomenon has been observed in both experimental (Davisson and Evans 1952, Hedgran and Hultberg 1954) and simulation studies (Brunner *et al* 2014, Somlai-Schweiger and Ziegler 2015). Although the timing derived from the scintillation photons can show small differences between the H2H and B2B configurations (Derenzo *et al* 2015), Cerenkov

photons should contribute more to the coincidence timing resolution in H2H measurements than in B2B measurements.

Coincidence measurements were also performed using a pair of $3 \times 3 \times 20$ mm^3 BGO crystals coupled with RGB-HD SiPMs and a pair of $2 \times 3 \times 2$ mm^3 BGO coupled with NUV-HD SiPMs, respectively. The RGB-HD SiPMs have much poorer PDE at the shorter wavelengths where the Cerenkov light is most abundant, therefore these SiPMs serve as a control and we would expect less difference between the H2H and B2B coincidence timing resolutions. The smaller BGO samples lead to less timing dispersion and more efficient light collection and indicate the timing resolution achievable in more optimal conditions.

2.3. Data analysis

For each coincidence event, digitized energy signals were integrated over a 3 μs time window and the resulting energy values histogrammed to form the energy spectrum. The photopeak region was first fitted with two Gaussians: one for a 511-keV gamma ray and the other for a 434-keV X-ray escape peak from bismuth (Szczesniak *et al* 2013). The photopeak position and energy resolution at 511 keV were calculated by fitting the 511-keV peak with one Gaussian. Coincidence events included in the full width at tenth maximum (FWTM) around the 511-keV photopeak were used for timing analysis. The time pick-offs were determined by leading edge thresholding after linear interpolation of the digitized timing signals. The time difference between the two time pick-offs was computed for all coincidence events and the collection of time difference values were histogrammed to form the timing spectrum. The coincidence resolving time (CRT) was defined as the full width at half maximum (FWHM) of the fitted curve of the timing spectrum. To obtain the CRT as a function of time pick-off threshold value in each measurement, CRTs were calculated for a range of threshold values from 1.0 mV to 45.0 mV in 0.1 mV steps.

3. Results and discussion

3.1. Energy performance

Figure 3 shows the energy spectra obtained with a $3 \times 3 \times 20$ mm^3 BGO crystal coupled with a NUV-HD SiPM, a $3 \times 3 \times 20$ mm^3 BGO crystal coupled with a RGB-HD SiPM, and a $2 \times 3 \times 2$ mm^3 BGO crystal coupled with a NUV-HD SiPM. In each energy spectrum, the green dotted line and two vertical dashed lines indicate the one Gaussian fitting of the 511-keV photopeak and the energy window used for timing analysis, respectively. The escape peak was more visible in the energy spectra obtained with the $2 \times 3 \times 2$ mm^3 BGO coupled with NUV-HD SiPMs. The photopeak position and energy resolution of one detector in each detector pair are shown in table 1. Short BGO and NUV-HD SiPMs showed better energy resolution than longer BGO and RGB-HD SiPMs, respectively. One of the reasons for worse energy resolution in RGB-HD SiPMs is higher dark-count rate in RGB-HD SiPMs compared to NUV-HD SiPMs (Piemonte *et al* 2013, Piemonte *et al* 2016). Although energy resolution was slightly degraded using the B2B configuration, there was no obvious difference between H2H and B2B configurations with respect to energy performance. Since the number of Cerenkov photons produced by 511-keV gamma interactions is very small, scintillation photons provide the majority of the energy information.

3.2. Timing performance

Figure 4(a) shows one of timing spectra measured with 3 × 3 × 20 mm^3 BGO crystals coupled to NUV-HD SiPMs at a threshold of 2.2 mV in the H2H measurements. Figure 4(b) shows the root-mean-square error (RMSE) of single Gaussian (blue dashed line) and Lorentz (green line) fitting to the timing spectra as a function of threshold in the H2H measurements with 3 × 3 × 20 mm^3 BGO coupled with NUV-HD SiPMs. The Lorentz function is defined by:

$$f(x) = \frac{a}{(x-b)^2+c}+d \quad (1)$$

where *a*, *b*, *c*, and *d* are free parameters of the fit. As shown in figure 4(a) and (b), the timing spectra, especially data from NUV-HD SiPMs, were much better fitted with a Lorentz function than a single Gaussian. At lower thresholds (<~20 mV), timing spectra from NUV-HD SiPMs were also well fitted by two Gaussians. However, the timing spectra at higher thresholds or obtained from RGB-HD SiPMs were poorly represented by two Gaussians. Therefore, all timing spectra were fitted with a Lorentz function throughout this study in order to fairly compare CRT (FWHM) and FWTM of all different BGO and SiPM pairs across the wide range of thresholds studied. The ratio of the FWTM to FWHM in each timing spectrum measured with 3 × 3 × 20 mm^3 BGO coupled with NUV-HD SiPM as a function of threshold is shown in figure 4(c). It was observed that the ratio was much higher at lower thresholds. Moreover, the ratio rapidly decreased as the threshold increased and then flattened. From these results, we can infer that photons with two different time distributions are detected: one from the scintillation process and the other from Cerenkov radiation. Promptly produced Cerenkov photons contribute to narrowing of the timing spectrum at lower thresholds, resulting in improvement in timing resolution. At higher thresholds, the signal from the Cerenkov photons is not sufficient to exceed the threshold and triggering is dominated by the scintillation photons. Strong evidence for the influence of Cerenkov photons are the differences observed in the ratio between H2H and B2B configurations. Although some contribution of Cerenkov photons is also seen in B2B measurements (gray line), the ratio is lower than that from H2H measurements (red line) at lower thresholds. This can be explained by the directional nature of Cerenkov radiation.

Figure 5 (a) and (b) show the CRT as a function of threshold measured from the 3 × 3 × 20 mm^3 BGO crystals coupled with NUV-HD and RGB-HD SiPMs, respectively. Each plot includes results of H2H (red line) and B2B (gray line) measurements. As shown in figure 5(a), CRT values from H2H measurements were much better than those from B2B measurements at lower thresholds. This agrees well with the pattern of the ratio of FWTM to FWHM in figure 4(c). Although the timing derived from the scintillation photons can also show small differences between the H2H and B2B configurations (Derenzo *et al* 2015), due to the different propagation velocities of scintillation light versus 511 keV photons inside the crystal, the timing differences between the H2H and B2B configurations are too large to be explained by this effect. Consequently, it appears that the coincidence timing resolution of BGO is considerably improved by detection of Cerenkov photons.

In results from BGO coupled with RGB-HD SiPMs (figure 5(b)), similar patterns from the influence of Cerenkov photons were also observed. However, since RGB-HD SiPMs have lower PDE at UV/blue wavelengths and slightly higher noise properties than NUV-HD SiPMs, the influence of Cerenkov photons is significantly less than with the NUV-HD SiPMs. This difference between the two SiPM types is further strong evidence for the role of the Cerenkov photons in the CRT measurements with the NUV-HD SiPMs as all other factors are constant.

Coincidence timing resolution was much improved in $2 \times 3 \times 2$ mm^3 BGO coupled with NUV-HD SiPMs. However, the difference between H2H and B2B measurements was small compared to that in $3 \times 3 \times 20$ mm^3 BGO. This can be explained by the fact that Cerenkov photons reflected by the top and lateral surfaces contribute more to the coincidence timing resolution in $2 \times 3 \times 2$ mm^3 BGO than in $3 \times 3 \times 20$ mm^3 BGO since the path length of the reflected Cerenkov photons is much shorter in $2 \times 3 \times 2$ mm^3 BGO. The best CRT values from each measurement are shown in table 2. We achieved best CRT values of ~270 ps from $2 \times 3 \times 2$ mm^3 BGO crystals and a value of ~560 ps from $3 \times 3 \times 20$ mm^3 BGO crystals relevant to the detector size used in clinical PET scanners. To our knowledge, these are the best CRT values reported for BGO to date.

As a final test, we evaluated the timing spectrum as a function of source position between the two crystals in the H2H measurements. Figure 6 shows the timing spectra measured with two $3 \times 3 \times 20$ mm^3 BGO crystals coupled with NUV-HD SiPMs, as a ^{22}Na point source was moved to three different positions between the detectors of −20 mm, 0 mm (center), and +30 mm. The CRT values at three different positions were 555 ps, 561 ps, and 553 ps, respectively. The three estimated source positions using the TOF information were −20.5 mm, +0.1 mm, and +31.2 mm, respectively. The fact that the timing spectrum shifts appropriately with the source location demonstrates that the timing resolution values measured here are not due to electronic triggering crosstalk between the two detectors.

4. Conclusions

Cerenkov photons produced by 511-keV gamma ray interactions were observed in BGO coupled with NUV-HD SiPMs and this combination produce outstanding coincidence timing resolutions for BGO crystals. Adequate energy information is simultaneously obtained from integration of the scintillation photons. BGO is a cost-effective and very efficient scintillator for PET and based on these results, BGO can be considered as a relevant scintillator for TOF PET scanners. Further improvements in timing are likely possible, especially if photodetectors with even better near UV/blue response can be developed.

Acknowledgments

This work was funded in part by NIH R35 CA197608 and NIH R01 EB019439. The authors want to thank Emilie Roncali, Julien Bec, and Steven Lucero at the University of California, Davis for many useful discussions. We also thank Radiation Monitoring Devices for measuring the emission spectrum of BGO in Figure 1.

References

Brunner SE, Gruber L, Marton J, Suzuki K, Hirtl A. Studies on the Cherenkov Effect for Improved Time Resolution of TOF-PET. IEEE Trans. Nucl. Sci. 2014; 61:443–7.

Davisson CM, Evans RD. Gamma-Ray Absorption Coefficients. Rev. Mod. Phys. 1952; 24:79–107.

DeGrado TR, Turkington TG, Williams JJ, Stearns CW, Hoffman JM, Coleman RE. Performance characteristics of a whole-body PET scanner. J. Nucl. Med. 1994; 35:1398–406. [PubMed: 8046501]

Derenzo SE, Choong WS, Moses WW. Monte Carlo calculations of PET coincidence timing: single and double-ended readout. Phys. Med. Biol. 2015; 60:7309–38. [PubMed: 26350162]

Dolenec R, Korpar S, Krizan P, Pestotnik R, Verdel N. The Performance of Silicon Photomultipliers in Cherenkov TOF PET. IEEE Trans. Nucl. Sci. 2016:1.

Gola A, Piemonte C, Tarolli A. Analog Circuit for Timing Measurements With Large Area SiPMs Coupled to LYSO Crystals. IEEE Trans. Nucl. Sci. 2013; 60:1296–302.

Hedgran A, Hultberg S. Angular Distribution of Photoelectrons from Gamma Radiation of 0.4 and 1.3 Mev. Physical Review. 1954; 94:498–9.

Humm JL, Rosenfeld A, Del Guerra A. From PET detectors to PET scanners. Eur. J. Nucl. Med. Mol. Imaging. 2003; 30:1574–97. [PubMed: 14579100]

Karp JS, Surti S, Daube-Witherspoon ME, Muehllehner G. Benefit of time-of-flight in PET: experimental and clinical results. J. Nucl. Med. 2008; 49:462–70. [PubMed: 18287269]

Korpar S, Dolenec R, Križan P, Pestotnik R, Stanovnik A. Study of TOF PET using Cherenkov light. Nucl. Instrum. Methods Phys. Res. A. 2011; 654:532–8.

Lecoq P, Auffray E, Brunner S, Hillemanns H, Jarron P, Knapitsch A, Meyer T, Powolny F. Factors Influencing Time Resolution of Scintillators and Ways to Improve Them. IEEE Trans. Nucl. Sci. 2010; 57:2411–6.

Melcher CL. Scintillation crystals for PET. J. Nucl. Med. 2000; 41:1051–5. [PubMed: 10855634]

Moses WW. Recent Advances and Future Advances in Time-of-Flight PET. Nucl. Instrum. Methods Phys. Res. A. 2007; 580:919–24. [PubMed: 18836513]

Pepin CM, Berard P, Perrot AL, Pepin C, Houde D, Lecomte R, Melcher CL, Dautet H. Properties of LYSO and recent LSO scintillators for phoswich PET detectors. IEEE Trans. Nucl. Sci. 2004; 51:789–95.

Piemonte C, Acerbi F, Ferri A, Gola A, Paternoster G, Regazzoni V, Zappala G, Zorzi N. Performance of NUV-HD Silicon Photomultiplier Technology. IEEE Trans. Electron Dev. 2016; 63:1111–6.

Piemonte C, Ferri A, Gola A, Pro T, Serra N, Tarolli A, Zorzi N. Characterization of the First FBK High-Density Cell Silicon Photomultiplier Technology. IEEE Trans. Electron Dev. 2013; 60:2567–73.

Rihua M, Liyuan Z, Ren-Yuan Z. Optical and Scintillation Properties of Inorganic Scintillators in High Energy Physics. IEEE Trans. Nucl. Sci. 2008; 55:2425–31.

Rota Kops E, Herzog H, Schmid A, Holte S, Feinendegen LE. Performance characteristics of an eight-ring whole body PET scanner. J. Comput. Assist. Tomogr. 1990; 14:437–45. [PubMed: 2186064]

Somlai-Schweiger I, Ziegler SI. CHERENCUBE: Concept definition and implementation challenges of a Cherenkov-based detector block for PET. Med Phys. 2015; 42:1825–35. [PubMed: 25832073]

Surti S. Update on time-of-flight PET imaging. J. Nucl. Med. 2015; 56:98–105. [PubMed: 25525181]

Szczesniak T, Kapusta M, Moszynski M, Grodzicka M, Szawlowski M, Wolski D, Baszak J, Zhang N. MPPC Arrays in PET Detectors With LSO and BGO Scintillators. IEEE Trans. Nucl. Sci. 2013; 60:1533–40.

Wienhard K, Dahlbom M, Eriksson L, Michel C, Bruckbauer T, Pietrzyk U, Heiss WD. The ECAT EXACT HR: performance of a new high resolution positron scanner. J. Comput. Assist. Tomogr. 1994; 18:110–8. [PubMed: 8282858]

Wienhard K, Eriksson L, Grootoonk S, Casey M, Pietrzyk U, Heiss WD. Performance evaluation of the positron scanner ECAT EXACT. J. Comput. Assist. Tomogr. 1992; 16:804–13. [PubMed: 1522276]

Williams RT, Ucer KB, LoPresti JL. In the first instants … ultrafast views of radiation effects. Radiat. Meas. 2001; 33:497–502.

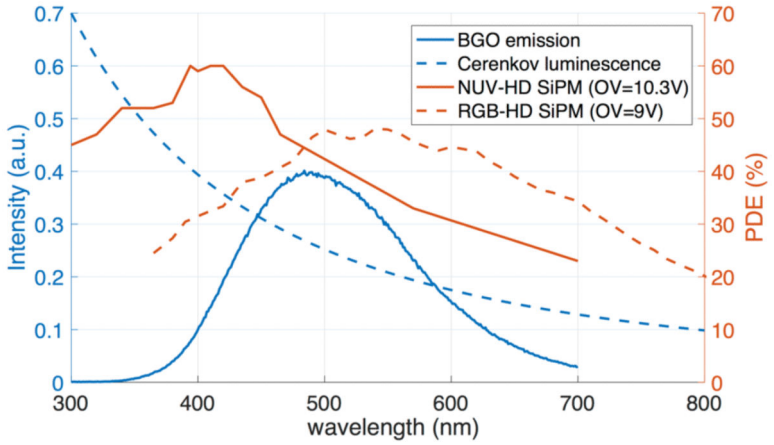

Figure 1.

PDE of NUV-HD (red) and RGB-HD (dashed red) SiPMs, emission spectrum of BGO (blue) and spectrum of Cerenkov luminescence (dashed blue) as a function of wavelength. BGO data courtesy of Radiation Monitoring Devices Inc, Watertown, MA.

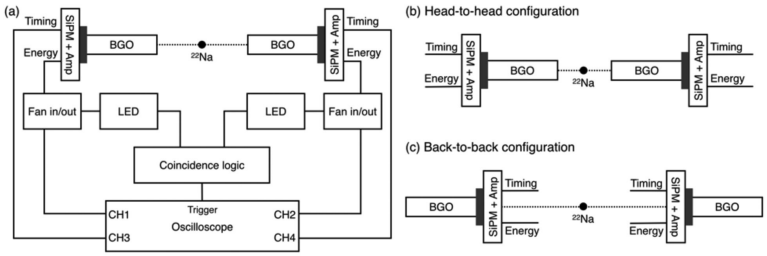

Figure 2.

Experimental setup for coincidence events (a). To examine the influence of Cerenkov photons, coincidence events were measured using head-to-head (b) and back-to-back (c) configurations.

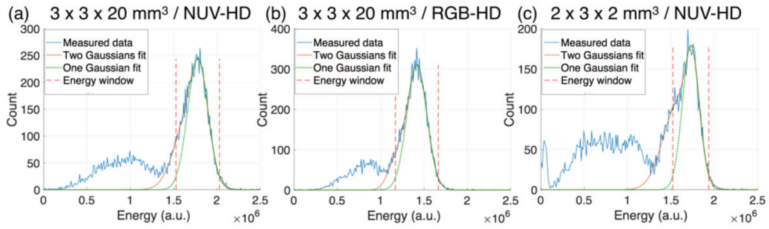

Figure 3.

Energy spectra obtained with 3 × 3 × 20 mm^3 BGO coupled with NUV-HD SiPM (a), 3 × 3 × 20 mm^3 BGO coupled with RGB-HD SiPM (b), and 2 × 3 × 2 mm^3 BGO coupled with NUV-HD SiPM (c).

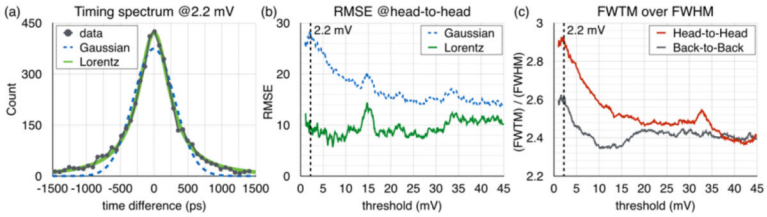

Figure 4.

Timing spectrum was measured at a threshold of 2.2 mV in the head-to-head measurements (a). The RMSE (b) and the ratio (c) of FWTM to FWHM in each timing spectrum were measured with $3 \times 3 \times 20$ mm^3 BGO crystals coupled with NUV-HD SiPMs as a function of threshold.

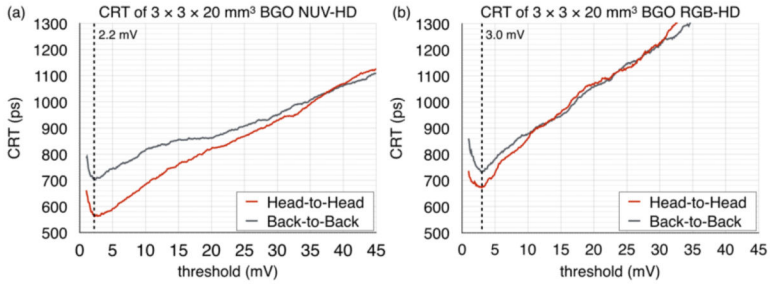

Figure 5.

CRT as a function of threshold measured from 3 × 3 × 20 mm^3 BGO coupled with NUV-HD (a) and RGB-HD (b) SiPMs.

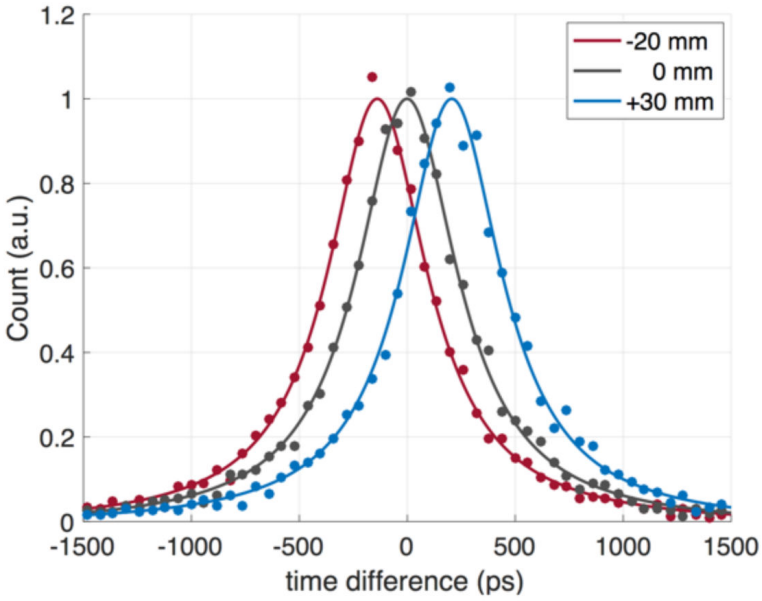

Figure 6.

Timing spectra measured with two 3 × 3 × 20 mm^3 BGO crystals coupled with NUV-HD SiPMs, using a ^{22}Na point source located at three different positions of −20 mm (red), 0 mm (gray), and +30 mm (blue) relative to the center point between the two crystals. The CRT values at three different positions were 555 ps, 561 ps, and 553 ps, respectively.

Table 1

Photopeak position and energy resolution for different BGO/SiPM combinations.

Pixel size (mm^3)	SiPM	Head-to-head		Back-to-back	
		Photopeak ($\times 10^6$)	Energy resolution	Photopeak ($\times 10^6$)	Energy resolution
3 × 3 × 20	NUV-HD	1.78	15.5%	1.76	16.4%
	RGB-HD	1.42	19.2%	1.42	20.0%
2 × 3 × 2	NUV-HD	1.73	13.2%	1.73	13.8%

Table 2

The best CRT values obtained from each measurement

Pixel size (mm^3)	SiPM	Threshold (mV)	CRT FWHM (ps)	
			Head-to-head	Back-to-back
3 × 3 × 20	NUV-HD	2.2	562	700
	RGB-HD	3.0	672	731
2 × 3 × 2	NUV-HD	2.2	267	277